# Characterization of Moisture Transport Properties of Cement-based Materials using Electrical Capacitance Tomography

Antti VOSS [1], Mohammad POUR-GHAZ [2], Marko VAUHKONEN [1], Aku SEPPÄNEN [1]

[1] University of Eastern Finland, Kuopio, Finland

[2] North Carolina State University, Raleigh, USA

Contact e-mail: antti.voss@uef.fi

ABSTRACT: The presence of moisture is the primary reason that causes the majority of physical and chemical damages in cement-based materials, and thus information on the temporal moisture condition and water movement properties is of great importance when assessing the durability of the material. This paper studies the ability of Electrical capacitance tomography (ECT) to visualize three-dimensional (3D) movement of water within mortar specimens. Additionally, we study the possibility to further use the ECT visualizations of moisture flows to estimate saturated hydraulic conductivity of the mortar. In the experiments, 3D and 1D unsaturated moisture flows were induced and ECT was applied to image the specimens during the ingress of water. For corroboration, the flow of moisture was also modeled numerically using finite element approximation of Richard's equation. The results show that ECT reconstructions are in good correspondence with the flow simulations. Moreover, the estimated saturated hydraulic conductivity of the mortar was close to the reference value determined with a separate test.

## 1 INTRODUCTION

Water, and aggressive agents transported with it are the main factors that initiate and speed up physical and chemical deterioration processes in cement-based materials. The durability of these materials is strongly related to their ability to impede flow of water (Monteiro et. al (2006), Neville (1996)). Hence understanding the movement of water within the materials is critical since typically initiation of a degradation process, e.g. reinforcing steel corrosion, requires a certain degree of saturation. Thus, information on moisture transport properties and internal moisture distribution is necessary when assessing or predicting the durability.

Traditional technique to monitor water ingress inside cement-based materials is gravimetric method which is based on weighting the specimen at different time intervals. This method provides information only on the amount of absorbed water but no information on how the water is spatially distributed inside the material. To approximate the spatial moisture distribution, the material could be sliced into smaller pieces and the moisture content of each piece could be then determined. This procedure, however, is inaccurate and destructive. More useful and accurate techniques to monitor the spatial water movement within cement-based materials are tomographic imaging modalities, including neutron imaging (Pleinert et al (1998), Zhang et. al (2011)), nuclear magnetic resonance imaging (Gummerson et. al (1979), Beyea et. al (1998)), X-ray (Roels et. al (2006), Pour-Ghaz et. al (2009)) and electrical resistance tomography (ERT) (Hallaji et. al (2015), du Plooy et. al (2013), Smyl et. al (2016)). However, these methods have limitations; for example, some of them are extremely expensive for operational use and are limited to small specimens and laboratory environment only. While ERT



License: https://creativecommons.org/licenses/by/4.0/

may not suffer from the above limitations, it is suitable only for imaging surface wet (electrically conductive) specimens.
Our recent studies have shown that in surface-dry cement-based materials, a suitable technique to monitor moisture ingress is Electrical Capacitance Tomography (ECT) (Voss et al. (2016,2018)), which is based on imaging the internal electrical permittivity distribution of the target on the basis of capacitance measurements obtained from the target's surface. In this paper, we apply ECT for imaging 3D unsaturated moisture flow in mortar specimen and compare the experimental results with simulated moisture content distributions obtained by finite element approximation of 3D Richard's equation which is a known unsaturated moisture flow model for porous media. The primary goal of this experiment is to demonstrate the feasibility of ECT to visualize the movement of water inside cement-based materials in 3D. Secondly, we study whether the ECT reconstructions could be further used for estimating material transport parameters experimentally. For the latter aim, we conduct another water ingress experiment where we induce a one-dimensional (1D) flow and use ECT to track the propagation of the 1D water front. This information provided by ECT is then combined with a simple 1D moisture flow model (Sharp Front- model) to estimate the saturated hydraulic conductivity of the mortar specimen which is a parameter that describes the ease of water movement through porous material.

## 2 MATERIALS AND METHODS

### *2.1 Electrical Capacitance Tomography*

In electrical capacitance tomography (ECT), the electrical capacitances are measured between electrodes that are placed on the surface of a target (Figure 1.). A commonly used measurement strategy is to excite one electrode at a time to some fixed potential while keeping all the other electrodes at earth and then measure the capacitances of the grounded electrodes with respect to the excited electrode. Based on this set of capacitance measurements, the internal electrical permittivity distribution $\epsilon(x)$ of the target is reconstructed.

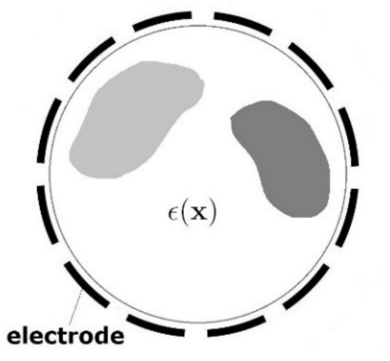


Figure 1. Schematic 2D ECT sensor setup.

The mathematical model describing the ECT measurements, also referred to as forward model, consist of a partial differential equation

$$\nabla \cdot \epsilon(x)\nabla u(x) = 0, \qquad x \in \mathrm{R}^3 \tag{1}$$

where $u(x)$ is electric potential, and moreover, the forward model includes boundary conditions for the electrode excitations and computation of the capacitances. When solving the forward model, the permittivity $\epsilon(x)$ and the electrode excitation potentials are known, and the task is to find out the electric potential $u(x)$ and the resulting inter-electrode capacitances. For more detailed description of the ECT's forward model and how to approximate its solution, e.g., using finite element method, see Voss et. al (2016), Rimpiläinen et. al (2011) and Watzenig (2009).

Contrary to the forward problem, reconstructing the electrical permittivity distribution based on noisy capacitance data is called an inverse problem. An estimate for the electrical permittivity is sought with the help of the forward model; find such a permittivity distribution that gives similar capacitance data than the actually measurements. However, the inverse problem of ECT is ill-posed which implies its classical solutions (e.g. least squares solutions) are non-unique and very sensitive to measurement and modeling errors. Hence, the solution of the inverse problem requires special methods. We note that the spatial resolution of ECT is relatively low due the severely ill-posed nature of the inverse problem. For general review of ill-posed inverse problems and methods to solve them, we refer to Kaipio and Somersalo (2006). In this work spatial smoothness promoting regularization is incorporated in the permittivity reconstructions. Furthermore, the solution of the inverse problem is solved in the difference imaging scheme where the changes in permittivity are estimated based on the difference in the ECT data between two time instants. In particular, the so-called sequentially linearized (SL) difference imaging method was applied to reconstruct the temporal permittivity changes caused by the flow of moisture. The SL difference imaging method is described in Voss et. al (2017).

### *2.2 Experimental setup*

Figures 3. (a)-(b) show the schematic experimental setups for the 3D and 1D water flow experiments, respectively. In the 3D case, a cylindrical water reservoir with a diameter of 2.5 cm was mounted off center on top of the specimen. To induce a 1D flow, larger water reservoir was used that covered the whole top surface of the mortar specimen. The mortar specimen used in both experiments was a cylinder with a diameter and height of 10.15 cm and 20.30 cm, respectively. The specimen was made with Portland cement type I/II and fine aggregate and had water-to-cement ratio (w/c) of 0.42. In both experiments the specimens were sealed to avoid evaporation and the duration of the water ingress experiments was 5 days.

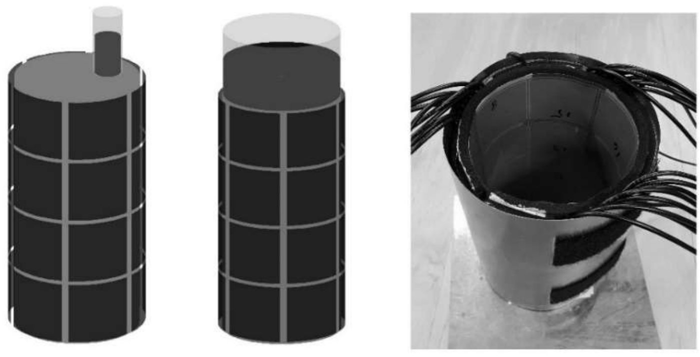

(a) (b) (c)

Figure 2. Illustrations of the experimental setups (a) 3D flow and (b) 1D flow. (c) A photo of the ECT sensor.

The ECT electrode fixture (Figure 3. (c)) included 24 electrodes that were made of flexible circuit board. The size of each electrode was 5.00 cm x 5.00 cm. An outer electrically grounded metal screen surrounded (excluding the top) the ECT electrode fixture to reduce the disturbances of the external electromagnetic fields. The capacitance data was continuously measured during the 5-day water ingress experiments using a commercial ECT measurement device.

### *2.3 Moisture flow simulation model*

The moisture ingress in the mortar specimens was modeled numerically by a finite element approximation of an unsaturated moisture flow model for porous media better known as Richard's equation (Richard (1931)). The flow model is of the form

$$\frac{\partial \theta}{\partial t} = \nabla \cdot K(\theta)\nabla h(\theta) \ , \qquad (2)$$

where $\theta$ ($m^3/m^3$), is volumetric moisture content, $K$ (m/s) is the unsaturated hydraulic conductivity and $h$ (m) is the pressure head. To simulate the moisture flow, $h(\theta)$ and $K(\theta)$ functions require experimental determination of water retention curve and saturated hydraulic conductivity ($K_s$) of the material. The saturated hydraulic conductivity of the mortar determined for the moisture simulations is also used as a reference value in the second part of this paper where we aim at estimating this parameter. The procedure to measure $K_s$ and the water retention curve and how to construct functions $h(\theta)$ and $K(\theta)$ we refer to papers Smyl et al. (2016) and Pour-Ghaz et. al (2009).

The equation (2) was numerically approximated using a commercial finite element software HYDRUS 3D (Šimunek, et. al (2012)). The following boundary conditions were applied: The part of the specimen that was in contact with water was modeled as fully saturated ($\theta_s$) (saturation moisture content was obtained from the water retention data). Elsewhere in the boundary a zero-flux boundary condition was applied.

### *2.4 Sharp Front – model*

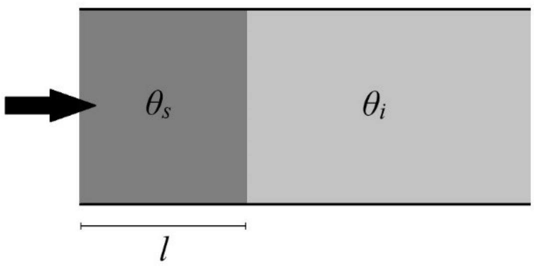


Figure 3. One-dimensional water absorption into a porous material – Sharp Front model.

Sharp front (SF) theory offers a mathematically simple formulation to model 1D absorption processes in porous materials (Hall and Hoff (2011)). The following model for 1D water front penetration, $l(t)$, in porous material (Figure 2.) can be derived based on SF theory

$$l = \left(\frac{2K_s h_e}{f_e}\right)^{1/2} t^{1/2}, \qquad (3)$$

where $K_s$ is the saturated hydraulic conductivity, $h_e$ is the effective water front pressure head, $f_e = \theta_s - \theta_i$ is the effective porosity and $t$ is time. The assumptions behind the equation (3) are: i) the flow is strictly 1D and the water front sharp ii) the wetted region is considered fully saturated ($\theta_s$) iii) the initial moisture content $\theta_i$ ahead of the water front is uniform. Moreover, all the model parameters ($K_s, h_e, f_e$) in the flow model are assumed to be unchanged throughout the flow process.

In the paper, we propose an approach to estimate $K_s$ of a mortar specimen using equation (3) and experimental water front penetration data provided by ECT imaging of a 1D flow process. To use this approach, the other two parameters, $h_e$ and $f_e$, need to be known. They are determined based on the known initial moisture content of the specimen and using the water retention data (Section 2.2); $f_e$ is straightforward and for calculation of $h_e$ see Neumann (1976). After the water front location as a function of time data has been obtained by ECT imaging, the task is to do a linear LS fit to data $(l, t^{1/2})$ and then using the slope of the fitted line an estimate for $K_s$ can be calculated according to equation (3).

# 3 RESULTS AND DISCUSSION

## *3.1 3D moisture flow*

Figure 4. shows the ECT-based 3D permittivity reconstructions and the simulated moisture content distributions at times 1, 2, 3, 4 and 5 day of the 3D water ingress. The propagation of moisture within the specimen is clearly indicated by the ECT reconstructions, and at any instant of time the reconstructed permittivity distributions are in good agreement with the simulated moisture content distributions. Although the comparison between the ECT results and moisture flow simulations is only qualitative (quantitative comparison would require a model between electrical permittivity and moisture content), it seems though that ECT offers a reliable imaging tool to visualize 3D moisture transport in cement-based materials.

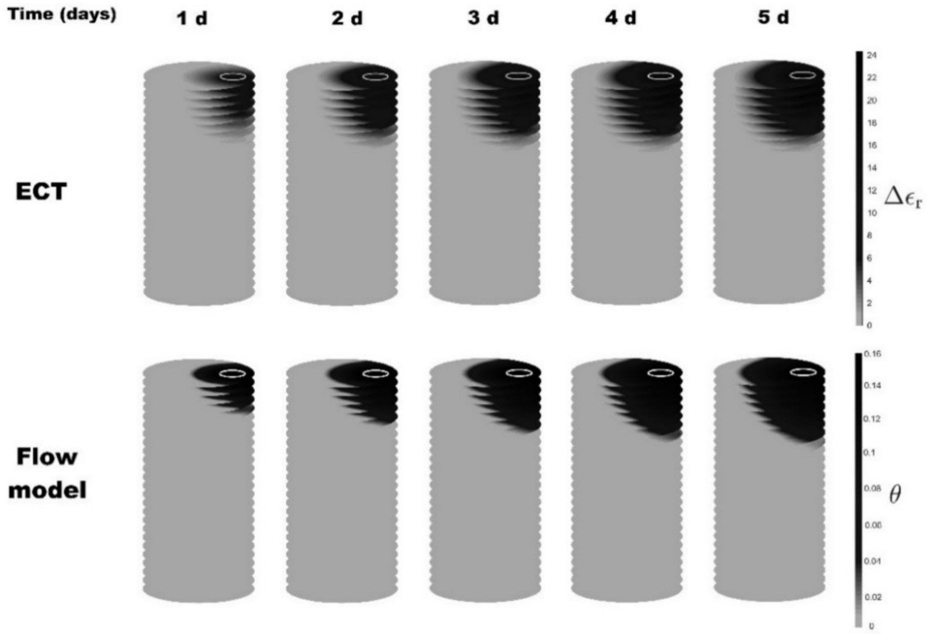


Figure 4. 3D ECT reconstructions and simulated moisture content distributions at different times of the 3D flow of moisture.

## *3.2 1D moisture flow and estimation of transport properties*

The 3D ECT reconstructions of the 1D flow experiment are shown in Figure 5. at times corresponding to 1, 2, 3, 4 and 5 day of water ingress. The simulated moisture content distributions are presented in the same figure at the respective times. Again, the correspondence between the ECT reconstructions and the modeled moisture distributions is relatively good.

However, the ECT reconstructions seem to slightly overestimate the spread of moisture compared to the flow simulations. This might be partly caused by the relatively low resolution of ECT, and partly due to the variation in transport properties between the specimens used in the actual 1D water ingress experiment and in the experiment to measure the simulation parameters. Despite the minor differences, the water front shows fairly consistent propagation in the ECT reconstructions. To improve the accuracy of ECT reconstructions, so-called absolute imaging scheme could be used instead of difference imaging, however, absolute imaging increases the computational complexity and time of the reconstructions, and it does not tolerate measurement and modeling errors as good as difference imaging does.

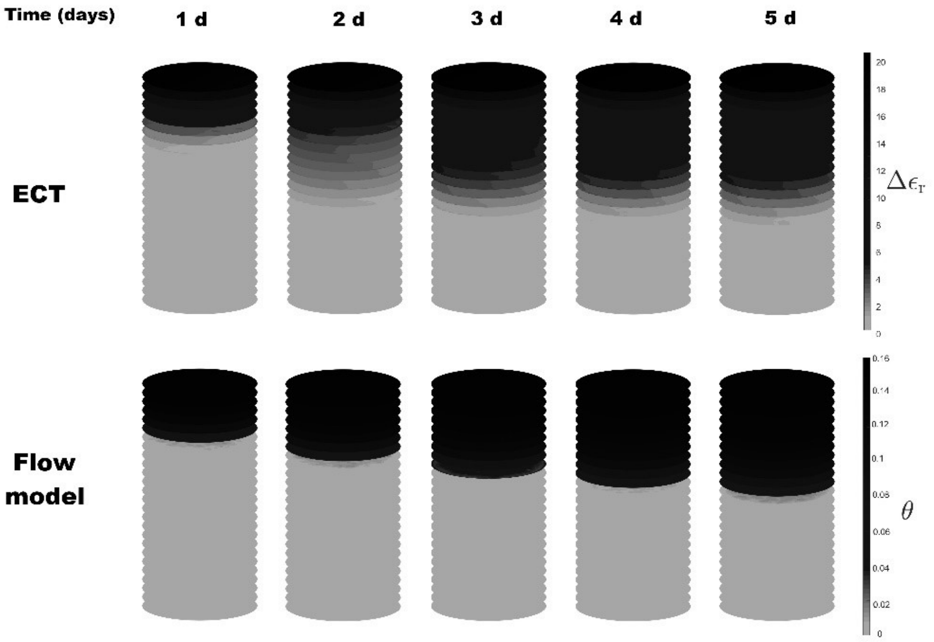


Figure 5. 3D ECT reconstructions and simulated moisture content distributions at different times of the 1D flow of moisture.

The water front penetration as a function of time was determined from the series of ECT reconstructions using a threshold permittivity value (more time instants were used than are shown in Figure 5.). The approximated water front locations are plotted as a function square root of time in Figure 6. According to SF-theory the $(l, t^{1/2})$ data points should fall into a straight line. Although individual data points in Figure 6. deviate from the predicted theory, the water front propagation in total shows linear increase. The use of absolute imaging methods, as stated above, would probably enable more accurate determination of the water front locations.

To estimate the saturated hydraulic conductivity, $K_s$, as described in Section 2.4, a linear LS fit was performed to the data $(l, t^{1/2})$ in Figure 6. The fitted line is also presented in Figure 6. Using the slope of the fitted line and the relation given by equation (3)

$$\text{slope} = \left(\frac{2K_s h_e}{f_e}\right)^{1/2} \quad (4)$$

an estimate for $K_s$ can be calculated. The estimated and reference values of $K_s$ are presented in Table 1. The estimated $K_s$, $4.30 \times 10^{-11}$ (m/s), is about 20 % higher than the reference value, but it can be considered a fairly reasonable estimate acknowledging all the possible sources of errors, for example, artefacts in the ECT reconstructions and uncertainty in the determination of the reference $K_S$. This result strengthens the feasibility of our proposed method to further use the ECT reconstructions of moisture flows to characterize moisture transport properties of cement-based materials.

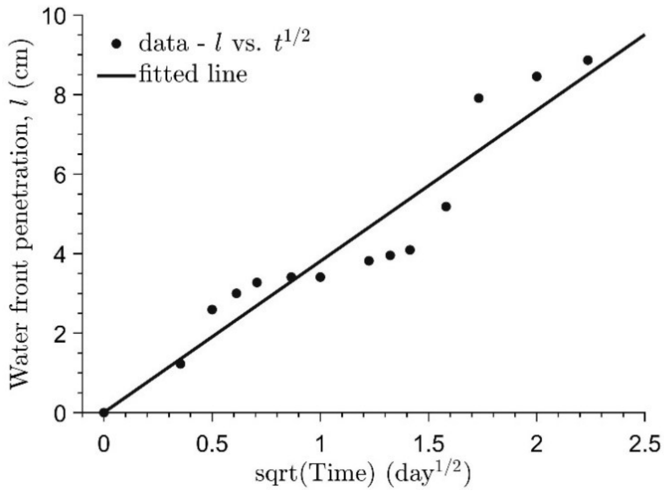


Figure 6. The water front penetration distance as a function of square root of time.

Table 1: Estimated and reference saturated hydraulic conductivity value for the mortar.

| Estimated $K_S$ (m/s) | Reference $K_S$ (m/s) |
|---|---|
| $4.30 \times 10^{-11}$ | $3.50 \times 10^{-11}$ |

## 4 SUMMARY AND CONCLUSIONS

In this work, we studied the ability of electrical capacitance tomography to monitor 3D water transport in mortar specimen. In addition, we investigated whether the ECT reconstructions of the moisture flow could be further utilized to estimate saturated hydraulic conductivity of the mortar when combining the information of ECT with a simple moisture flow model. In the experiments, ECT was applied to mortar specimens to monitor the induced unsaturated ingress of moisture inside them. The results show that ECT can image 3D moisture transport within the mortar specimen with a reasonable accuracy when compared to numerical moisture flow simulations. Moreover, the estimated hydraulic conductivity of the mortar was in good correspondence with the value determined with a separate test. ECT shows potential for becoming a tool for imaging three-dimensionally distributed moisture distributions in cement-based materials and possibly even characterizing their moisture transport properties.

## 5 ACKNOWLEDGEMENTS

This work was supported by the European Union‘s Horizon 2020 research and innovation programme under grant agreement No 764810.

# 6 REFERENCES


Beyea, S, Balcom, B, Bremner, T, Prado, P, Green, D, Amstrong, R, Grattan-Bellew, P, 1998, Magnetic resonance imaging and moise content profiles of drying concrete, *Cement and Concrete Research*, 28(3), 453-463.

du Plooy, R, Villain, G, Palma Lopes, S, Ihamouten, A, Derobert, X, Thauvin, B, 2013, Electromagnetic non-destructive evaluation techniques for the monitoring of water and chloride ingress into concrete: a comparative study, *Materials and Structures,* 48(1-2), 369-386.

Gummerson, RJ, Hall, C, Hoff, WD, Hawkes, R, Holland, GN, Moore, WS, 1979, Unsaturated water flow within porous materials observed by NMR imaging, *Nature,* 218, 56-57.

Hall, C, Hoff, WD, 2011Water Transport in Brick, Stone and Concrete*, 2nd Edition*. Taylor & Francis.

Hallaji, M, Seppänen, A, Pour-Ghaz, M, 2015, Electrical resistance tomography to monitor unsaturated moisture flow in cementitious materials, *Cement and Concrete Research*, 69, 10-18.

Kaipio, JP, Somersalo, E, 2005, *Statistical and Computational Inverse Problems, 2nd Edition*. Springer.

Monteiro, PJM, Mehta, PK, 2006, *Concrete Microstructure, Properties and Materials, 3rd Edition*. McGraw-Hill.

Neumann, SP, 1976, Wetting front pressure head in the infiltration model of Green and Ampt, *Water Resources Research*, 12(3), 564-566.

Neville, A, 1996, *Properties of Concrete, 4th Edition*. New York, Wiley.

Pleinert, H, Sadouki, H, Wittman, FH, 1998, Determination of moisture distributions in porous building materials by neutron transmission analysis, *Materials and Structures*, 31(4), 218-224.

Pour-Ghaz, M, Rajabipour, F, Couch, J, Weiss, J, 2009, Numerical and experimental assessment of unsaturated fluid transport in saw-cut (notched) concrete elements, *ACI Special Publication*, SP266-06 266, 73-86.

Richards, LA, 1931, Capillary conduction of liquids through porous mediums, *Physics 1*, 5, 318-333.

Rimpiläinen, V, Poutiainen, S, Heikkinen, LM, Savolainen, T, Vauhkonen, M, Ketolainen, J, 2011, Electrical capacitance tomography as a monitoring tool for high-shear mixing and granulation, *Chemical Engineering Science*, 66(18), 220-234.

Roels, S, Carmeliet, J, 2006, Analysis of moisture flow in porous materials using microfocus x-ray radiography, *International Journal of Mass and Heat Transfer*, 49(25), 4762-4772.

Šimunek, J, Van Genuchten, MT, Šejna, M, 2012, The HYDRUS software package for simulating the two-and three-dimensional movement of water, heat, and multiple solutes in variably-saturated porous media, *Technical manual*, 2, 258.

Smyl, D, Hallaji, M, Seppänen, A, Pour-Ghaz, M, 2016, Quantitative electrical imaging of three-dimensional moisture flow in cement-based materials, *International Journal of Mass and Heat Transfer*, 103, 1348-1358.

Voss, A, Pour-Ghaz, M, Vauhkonen, M, Seppänen, A, 2016, Electrical capacitance tomography to monitor unsaturated water ingress in cement-based materials, *Cement and Concrete Research*, 89, 158-167.

Voss, A, Pour-Ghaz, M, Vauhkonen, M, Seppänen, A, 2017, Difference reconstruction methods for electrical capacitance tomography imaging of two-dimensional moisture flow in concrete, *in the 9th International Conference on Inverse Problems in Engineering (ICIPE)*, Waterloo, Canada.

Voss, A, Hänninen, N, Pour-Ghaz, M, Vauhkonen, M, Seppänen, A, 2018, Imaging of two-dimensional unsaturated moisture flows in uncracked and cracked cement-based materials using electrical capacitance tomography, *Materials and Structures*, 51(3), 68.

Watzenig, D, Fox, C, 2009, A review of statistical modelling and inference for electrical capacitance tomography, *Measurement Science and Technology*, 20(5), 052002.

Zhang, P, Wittman, FH, Zhao, TJ, Lehmann, EH, Vontobel, P, 2011, Neutron radiography, a powerful method to determine time-dependent moisture distributions in concrete, *Nuclear Engineering and Design*, 241(12), 4758-4766.